



BNL-95200-2011-BC

***Composite Materials under Extreme Radiation and
Temperature Environments of the Next Generation
Nuclear Reactors***

Nicholas Simos

Composite Materials / Book 2
InTECH Open Access Publisher

Submitted March 25, 2011

Physics Department

Brookhaven National Laboratory

**U.S. Department of Energy
DOE Office of Science**

Notice: This manuscript has been authored by employees of Brookhaven Science Associates, LLC under Contract No. DE-AC02-98CH10886 with the U.S. Department of Energy. The publisher by accepting the manuscript for publication acknowledges that the United States Government retains a non-exclusive, paid-up, irrevocable, world-wide license to publish or reproduce the published form of this manuscript, or allow others to do so, for United States Government purposes.

This preprint is intended for publication in a journal or proceedings. Since changes may be made before publication, it may not be cited or reproduced without the author's permission.

DISCLAIMER

This report was prepared as an account of work sponsored by an agency of the United States Government. Neither the United States Government nor any agency thereof, nor any of their employees, nor any of their contractors, subcontractors, or their employees, makes any warranty, express or implied, or assumes any legal liability or responsibility for the accuracy, completeness, or any third party's use or the results of such use of any information, apparatus, product, or process disclosed, or represents that its use would not infringe privately owned rights. Reference herein to any specific commercial product, process, or service by trade name, trademark, manufacturer, or otherwise, does not necessarily constitute or imply its endorsement, recommendation, or favoring by the United States Government or any agency thereof or its contractors or subcontractors. The views and opinions of authors expressed herein do not necessarily state or reflect those of the United States Government or any agency thereof.

Composite Materials under Extreme Radiation
and Temperature Environments of the Next
Generation Nuclear Reactors

Nicholas Simos
Brookhaven National Laboratory
USA

1. Introduction

In the nuclear energy renaissance, driven by fission reactor concepts utilizing very high temperatures and fast neutron spectra, materials with enhanced performance that exceeds are expected to play a central role. With the operating temperatures of the Generation III reactors bringing the classical reactor materials close to their performance limits there is an urgent need to develop and qualify new alloys and composites. Efforts have been focused on the intricate relations and the high demands placed on materials at the anticipated extreme states within the next generation fusion and fission reactors which combine high radiation fluxes, elevated temperatures and aggressive environments. While nuclear reactors have been in operation for several decades, the structural materials associated with the next generation options need to endure much higher temperatures (1200°C), higher neutron doses (tens of displacements per atom, dpa), and extremely corrosive environments, which are beyond the experience on materials accumulated to-date. The most important consideration is the performance and reliability of structural materials for both in-core and out-of-core functions.

While there exists a great body of nuclear materials research and operating experience/performance from fission reactors where epithermal and thermal neutrons interact with materials and alter their physio-mechanical properties, a process that is well understood by now, there are no operating or even experimental facilities that will facilitate the extreme conditions of flux and temperature anticipated and thus provide insights into the behaviour of these well understood materials. Materials, however, still need to be developed and their interaction and damage potential or lifetime to be quantified for the next generation nuclear energy. Based on material development advances, composites, and in particular ceramic composites, seem to inherently possess properties suitable for key functions within the operating envelope of both fission and fusion reactors. In advanced fission reactors composite materials are being designed in an effort to extend the life and improve the reliability of fuel rod cladding as well as structural materials. Composites are being considered for use as core internals in the next generation of gas-cooled reactors. Further, next-generation plasma-fusion reactors, such as the International Thermonuclear Experimental Reactor (ITER) will rely on the capabilities of advanced composites to safely withstand extremely high neutron fluxes while providing superior thermal shock resistance.

1 In addition it will be required by the composite to possess and maintain under severe
2 neutron irradiation extremely high thermal conductivity to enable the flow of the
3 anticipated extreme thermal heat loads generated in the core. The first wall and blanket
4 surrounding the core in the fusion reactor are the two elements where composites are
5 considered leading candidates.

6 Composites of special interest to both fission and fusion next generation nuclear reactors are
7 carbon-fiber (C/C) and silicon carbide fiber (SiC_f/SiC), and more recently, C/SiC
8 composites. These are continuous fiber-reinforced materials of either carbon or silicon
9 carbide fibers infiltrated with a similar matrix. During the last two decades a number of
10 studies have been conducted to address the feasibility and response of the two composites
11 to different radiation environments of fission and fusion reactors and identify their
12 limitations. While these composite structures have a significant advantage over materials
13 used in the same reactor applications (i.e. nuclear graphite, BeO and metal alloys) because of
14 the physical and mechanical properties they possess, they also experience limitations that
15 require quantification. Carbon-fiber composites for example while they can have
16 customized architecture to enhance desired properties, such as thermal conductivity, they
17 too may experience anisotropic dimensional changes and be susceptible to irradiation-
18 induced degradation. SiC_f/SiC composites, on the other hand exhibit good fracture
19 resistance and low induced activity due to the irradiation stability of the SiC crystal but their
20 technology is less mature. Critical issues such as cost, fabrication and joining as well as
21 uncertainties due to lack of experience data in performance/survivability and lifetime in the
22 combined extremes of high temperature and high fast neutron fluxes require further
23 evaluation to qualify and quantify their performance.

24 During the last three decades and driven primarily by the fusion reactor needs (i.e. ITER) a
25 extensive array of neutron-irradiation experiments at high temperatures have been
26 conducted using available test reactors while the technology in composites was maturing.
27 Facilities such as the High Flux Isotope Reactor (HFIR) at Oak Ridge National Laboratory,
28 Japan Materials Testing Reactor (JMTR) as well as test reactors in Europe have been used to
29 irradiate newly developed alloys and composites to anticipated fluence levels in the next
30 generation fusion and fission reactors. As mentioned above, the understanding of the
31 behaviour of reactor materials through studies and experience from the operating low
32 energy neutron reactors may not necessarily transfer to the new materials under a different
33 neutron spectrum. While the peak of the energy spectrum in the fission reactors to-date is ~1
34 MeV, neutrons in fast-spectrum reactors of the next generation are of several MeV while
35 neutrons from fusion reactions will have energies of ~14 MeV. Based purely on modelling it
36 is anticipated that the induced damage in the microstructure of materials will be similar to
37 the one corresponding to that induced by less than 1 MeV neutrons. While the assumption
38 may be generally correct, there is greater uncertainty with composites which do not form a
39 perfectly oriented structure and are subject to the effects of dissimilar response between the
40 fibre structure and the matrix. In addition, interaction with higher energy neutrons will
41 generate more hydrogen and helium (as a result of nuclear interactions and transmutation
42 products). Helium trapped within basal graphite planes and irradiation-induced defects will
43 form bubbles and degrade the microstructure of the constituents. Therefore understanding
44 how these composite structures behave in the fast neutron environment and what the
45 degradation rate of their key properties (thermal conductivity, expansion, strength, etc.) is
46 important and assessment by means of extrapolation from available data will be risky.

1 To observe the effects of high energy irradiating particles on composite structures,
2 irradiation studies have been launched using the Brookhaven National Laboratory (BNL)
3 proton linear accelerator and the target station at the isotope production facility (BLIP). The
4 tuneable, ~25 kW (~110 μ A peak) accelerator can accelerate protons to energies up to 200
5 MeV. Irradiation damage studies on graphite, carbon composites and new alloys have been
6 performed in different phases using the proton beam directly on the materials and reaching
7 fluences of $\sim 10^{21}$ protons/cm². Results on the finding following proton irradiations on
8 carbon composites, graphite and composite-like structures are presented in subsequent
9 sections. In a different irradiation mode where the isotope targets completely absorb the 116
10 MeV protons, a mostly isotropic fast neutron is generated downstream of the isotope targets
11 from the spallation process. This neutron spectrum with mean energy of ~ 9 MeV is utilized
12 for the irradiation of composites and new alloys. While peak fluences are of the order of 10^{19}
13 - 10^{20} neutron/cm² for each yearly proton beam run (much lower than the $\sim 10^{21}$ - 10^{22} n/cm²)
14 expected in the fusion reactor, still the interaction of these new composites with
15 predominantly fast neutrons is expected to provide useful indicators of their stability and
16 resilience to damage. Neutron irradiation studies at BNL BLIP have been completed recently
17 for a number of super alloys and nano-structured coatings (Al_2O_3 , TiO_2) on various
18 substrates. Nanostructured coatings, along with AlBeMet, an aluminium-beryllium metal
19 matrix composite, and structures made of fusion-bonded dissimilar materials constitute a
20 special class of composites which are discussed in a subsequent section.

21 **2. Composites and extreme environments**

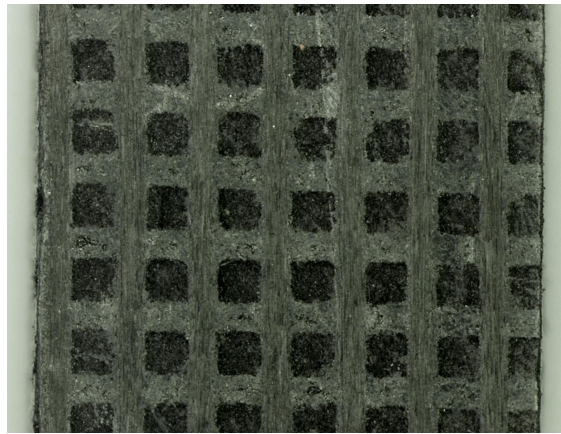
22 The development of advanced materials to be used in next generation reactors (Zinkle, 2004)
23 has been driven by the need to endure the extreme environment consisting of prolonged,
24 highly damaging radiation fluxes (tens of dpa), extreme temperatures (above 1000°C and up
25 to 1200°C) and high stress conditions, which together can push well-understood and widely
26 used materials beyond their limit. In fusion and fission reactor applications there are certain
27 key properties that the materials which are playing a pivotal role (i.e. first wall and blanket
28 in a fusion reactor) must maintain. These include low activation, structural integrity,
29 dimensional stability, thermal conductivity and inherent ability to absorb thermal shock.

30 **2.1 C/C composites**

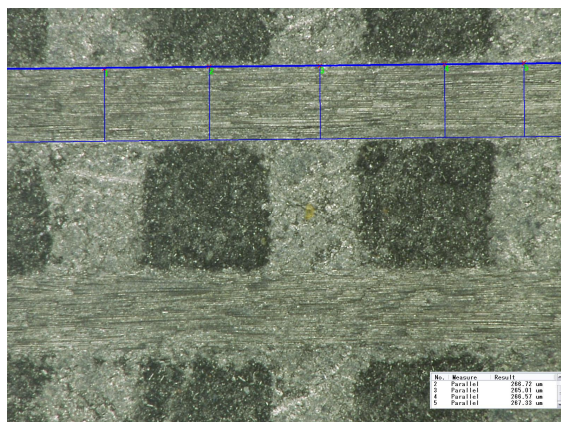
31 Carbon fibre reinforced composites (C_f/C) are an attractive choice for use in the extreme
32 environment of the next generation reactors because of some key properties they inherently
33 possess, namely enhanced strength as compared to nuclear graphite, thermal shock
34 resistance because of their unique structure, extremely low thermal expansion, enhanced
35 thermal conductivity due to the presence and directionality of fibres and low neutron
36 activation. Due to their attractive properties carbon-carbon composites have enjoyed
37 widespread use in advanced technologies which have led to the maturity of their technology
38 and fabrication. A wide variety of architectures of the fibre/matrix have been developed as
39 well as fabrication techniques. Most widely used architectures are the two-dimensional (2D
40 C_f/C) and three-dimensions (3D C_f/C) forms. Shown in Figures 1 and 2 are sections of the
41 three-dimensional architecture of the composite (FSI 3D C_f/C) indicating the orderly fibre
42 bundle (thickness of $\sim 265\mu\text{m}$) and matrix arrangement.

43 While carbon composites exhibit enhanced properties when compared to graphite,
44 radiation-induced damage from neutrons or other energetic particles such as protons is far
45 less well understood. To the contrary, nuclear graphite has been extensively studied for

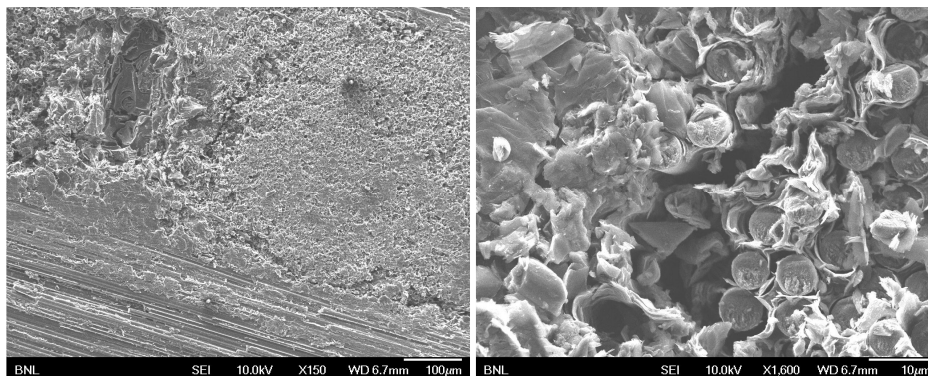
1 radiation-induced degradation for almost sixty (60) years and so the degradation of the key
 2 properties as a function of the neutron fluence such as thermal conductivity, dimensional
 3 stability and strength has been established thus leading to limitation thresholds for its use in
 4 more extreme environments (Gittus, 1975; Maruyama & Harayama 1992; Nikolaenko et al.
 5 1999). Key findings from these studies on graphite are the anisotropic dimensional changes
 6 that take place at higher radiation doses and most importantly the degradation of the
 7 thermal conductivity. Within the last two decades a body of experimental research work on
 8 irradiation damage of carbon-carbon composites has been reported prompted primarily by
 9 the need to identify higher performance, low neutron activation for the first wall of fusion
 10 reactors such as the International Thermonuclear Experimental Reactor (ITER). Of primary
 11 interest in these reported studies (Burchell, 1992, 1994; Burchell et al. 1996; Barabash, et al.,
 12 1998) are neutron irradiation induced dimensional changes, thermal conductivity and
 13 mechanical properties.
 14



15
 16 Fig. 1. Image of a 3D C_f/C composite structure using an optical microscope. Shown is the
 17 orderly arrangement of the fibre bundles and the matrix
 18



19
 20 Fig. 2. A closer view of the fibre/matrix configuration of the 3D C_f/C composite and
 21 measured fibre bundle thicknesses



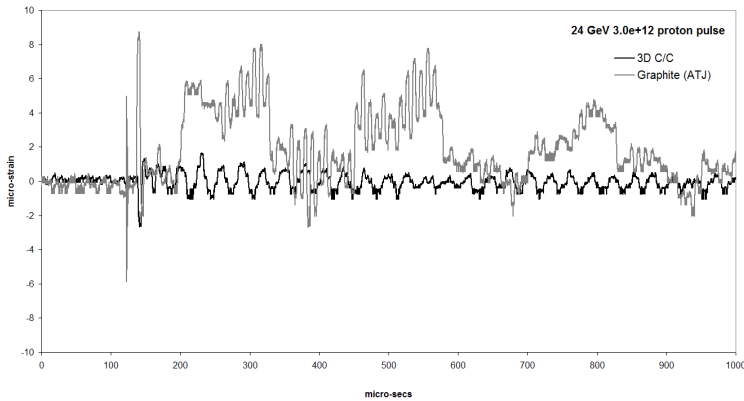
1
2 Fig. 3. SEM image of the matrix/fibre bundle interface in 3D C/C composite including the
3 presence of voids (left) and closer depiction (right) of one of the pre-existing voids,
4 individual fibres and interface

5 2.1.1 Shock resistance

6 One of the important attributes of C/C composites in the fusion reactor environment is their
7 inherent ability to absorb thermal shock. In an effort to quantify the ability of the C/C
8 composite to absorb thermal shock and so be used as the material of choice in a number of
9 high power accelerator applications including accelerator targets for the Long Baseline
10 Neutrino Experiment, Neutrino Factory (LBNE), beam collimating elements for the Large
11 Hadron Collider (LHC) or energetic beam absorbers, experiments have been performed
12 using intense pulses of energetic protons. In these experiments (Simos et al., 2005)
13 performed using the 24 GeV proton beam at the Accelerating Gradient Synchrotron (AGS)
14 at BNL the shock performance of FMI 3D C/C composite targets (16-cm long, 1-cm diameter
15 rods) was measured and compared to that of ATJ graphite. Shown in Figure 4 is the shock
16 test arrangement where 3D C/C composite and ATG graphite targets are instrumented with
17 fibre-optic strain gauges mounted on the surface of the target and measuring extremely fast
18 axial strain transients in the target resulting from its interaction with the 24 GeV proton
19 beam. The response from the intense (3.0×10^{12} protons) and focussed ($0.3\text{mm} \times 0.7\text{mm}$)
20 proton pulses on the ATJ graphite and 3D C/C targets is shown in Figure 5 where the two
21 are compared. It is evident from the comparison that the carbon-carbon composite shows a
22 much lower response to the shock induced by the beam while radial reverberations
23 indicated by the high frequency cycles within each axial cycle are damped out as a result of
24 the impedance interfaces (fibre/matrix) and the voids that are present as shown in Figure 3.
25 Due the potential implications and applications of high shock resistance in the carbon-
26 carbon composites which stem from the “effective” low thermal expansion coefficient
27 specific studies (Hereil, 1997) have focussed on experimentally verifying the compressive
28 wave velocities in a plate-impact configuration by wave decomposition. As observed in
29 (Simos et al., 2006; Hereil et al, 1997) the problem of shock in materials such as C/C remains
30 very complex due to the anisotropy and the fibre-matrix interfaces as well as the response to
31 dynamic loads of wave propagation in the individual components. In such materials,
32 understanding the behaviour at the mesoscale is important for modelling and
33 implementation of these composites in large-scale designs.



1
2 Fig. 4. C/C composite and ATJ graphite target shock test arrangement for the BNL AGS
3 proton beam tests
4

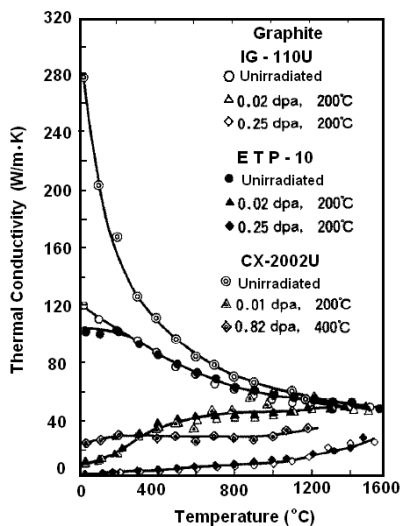


5
6 Fig. 5. Comparison of shock response in terms of axial strain recorded on 3D C/C and ATJ
7 graphite targets

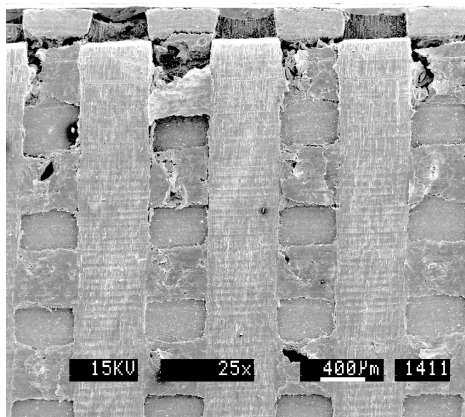
8 2.1.2 Radiation damage

9 While radiation damage in the carbon-carbon composites have been studied using neutrons
10 from various reactors such as the High Flux Isotope Reactor (HFIR) at Oak Ridge National
11 Laboratory or the Japan Materials Testing Reactor (JMTR), the radiation damage from very
12 energetic accelerator protons is very limited. Reported in the neutron-induced damage
13 studies (Burchell, 1992, 1996; Bonal et al., 2009) is that the composite undergoes dimensional
14 changes as a function of the fluence (or dpa) with the 3D architecture to exhibit an isotropic
15 behaviour. Under neutron irradiation and for a fluence of 1.0 dpa the thermal conductivity
16 reduces by ~50% (Burchell, 1992) while other studies (Maruyama & Harayama 1992) on CX-
17 2002U carbon-carbon composite suggest (see Figure 6) that there is a dramatic drop of the
18 thermal conductivity even at very low fluences (0.01 dpa) when the irradiation temperature
19 is 200°C and below the threshold where induced vacancies and interstitials become mobile.

1 Initiation of the degradation of the 3D C/C structure following neutron irradiation have
 2 been observed (Snead, 2004) and (Bonal et al, 2009) at the 2 dpa dose level leading to serious
 3 structural disintegration at about 10 dpa. These reported levels of irradiation damage onset
 4 pose a serious limitation on the desired lifetime of C/C plasma facing components in the
 5 fusion reactors.
 6



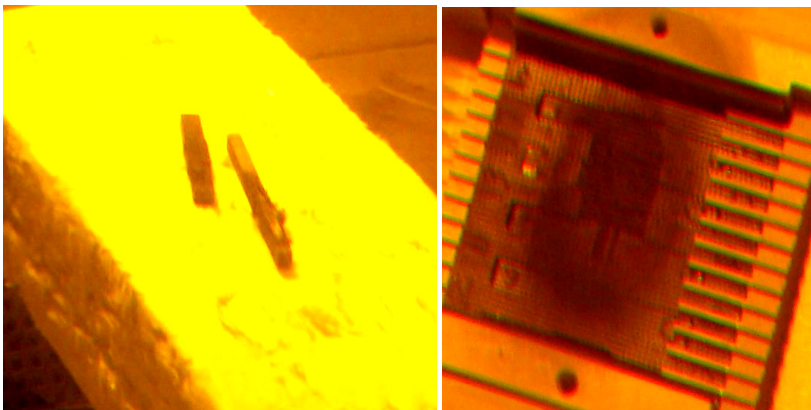
7
 8 Fig. 6. Thermal conductivity of neutron-irradiated graphite and carbon-carbon composite
 9 (Maruyama, 1992)



10
 11 Fig. 7. C/C composite following irradiation (10 dpa at 800 °C) showing serious degradations
 12 and anisotropic dimensional change in the form of swelling and shrinkage of fibre bundles
 13 (Snead, 2004)

14 For high power accelerators, while the thermal shock resistance is superior to graphite and
 15 so is the retention of thermal conductivity, degradation as a result of energetic proton

1 irradiation can be a serious limiting factor along with the dimensional stability required of
2 critical elements such as primary beam intercepting accelerator target and collimators.
3 Irradiation damage studies have been conducted in recent years (Simos et al, 2006a, 2006b,
4 2008) using the BNL 200 MeV Linac beam at the isotope production facility (BLIP). The main
5 objective was to assess the proton-induced damage at energies higher than the thermal and
6 fast neutrons these composite structures have been exposed in test reactors like HFIR and
7 JMTR and qualify the differences stemming from the irradiating species (protons vs.
8 neutrons) and energies (neutron energies a few MEV and proton energies up to 200 MeV).
9 Two architectural types of the composite were proton-irradiated and studied. A 2D C/C
10 structure (AC-200) made by Toyo Tanso to be used as a primary beam collimating material
11 at the Large Hadron Collider at CERN where 3.5 TeV protons at the beam halo ($>6\sigma$) will be
12 intercepted and diverted away from the circulating beam and a 3D C/C architecture made
13 by FMI as a target candidate material for the high power accelerators (LBNE and Neutrino
14 Factory). In the case of the 2-D C/C, dimensional stability in the direction along the fibres
15 was extremely important and so was the thermal conductivity and structural degradation
16 resistance. The first in series of long exposures ($>10^{20}$ p/cm² or >0.2 dpa) for these two
17 composites revealed that both architectures experience serious structural degradation.
18 Shown in Figure 8 is the structural degradation of the AC-200 2D C/C of specimens formed
19 normal to the fibre planes and along the fibres. Also shown in Figure 8 (right) is the
20 structural degradation of the FME 3D C/C composite. The peak proton fluence within the
21 damage area is $\sim 5.0 - 7.0 \cdot 10^{20}$ p/cm² ($\sim 0.6-0.8$ dpa) a level significantly lower than the one
22 associated with neutron-based irradiation of 2 dpa (Bonafant et al, 2009). Subsequent
23 irradiations to similar fluence thresholds verified the damage initiation onset at these low
24 proton fluences. Recent studies of the FMI 3D C/C composite irradiated in an inert gas
25 (argon) environment showed that there exists an environmental factor associated with the
26 damage given that the apparent fluence threshold for structural degradation has increased
27 slightly. Further investigation on this finding is currently under way.
28



29
30 Fig. 8. Irradiation damage induced by 200 MeV (left) protons on AC-200 2D C/C (left) and
31 damage induced by 160 MeV protons on FMI 3D C/C composite

32 The dimensional stability of the proton-irradiated 2D and 3D carbon composites was
33 measured using a LINSEIS high precision dilatometer in the BNL hot cell facility. Of

primary interest were the irradiation effects on the thermal expansion coefficient which represents a crucial parameter in the accelerator applications discussed above. From the precise measurements made it was observed that the fibres in both architectures undergo shrinkage as a result of the irradiation. This is evident in dimensional change data depicted in Figure 9 (left). The 2D C/C in its un-irradiated state will shrink along the directions of the fibres (negative thermal expansion) and expand in the direction normal to the fibre planes acting more like typical graphite. Following irradiation, however, and during the first thermal cycle that was applied to the 2-D specimen made along the fibres there is an accelerated expansion beyond the irradiation temperature (irradiation temperature is depicted as the inflection point in the curve). This is the result of the expansion of the fibres which experienced shrinking during irradiation. Interesting to note is that the composite with progressive upper temperature limit in a series of thermal cycles restores the un-irradiated behaviour up to that temperature. Observing the dimensional change along the normal direction shown in Figure 9 as a function of fluence one notes the growth that has occurred along the direction due to irradiation indicated by the apparent shrinkage during the thermal cycle when the composite is being restored towards the original configuration rather than expand with increasing temperature. This is evident in Figure 10 (left) which depicts a subsequent thermal cycle where the dimensional behaviour is aiming towards that of the un-irradiated composite. Comparing this restoration along the normal direction with that of irradiated IG-43 graphite, Figure 10 (right), the similarities can be seen which should be anticipated along this normal direction except that for the 2D C/C the growth in the lattice between the planes has occurred at lower irradiation temperatures.

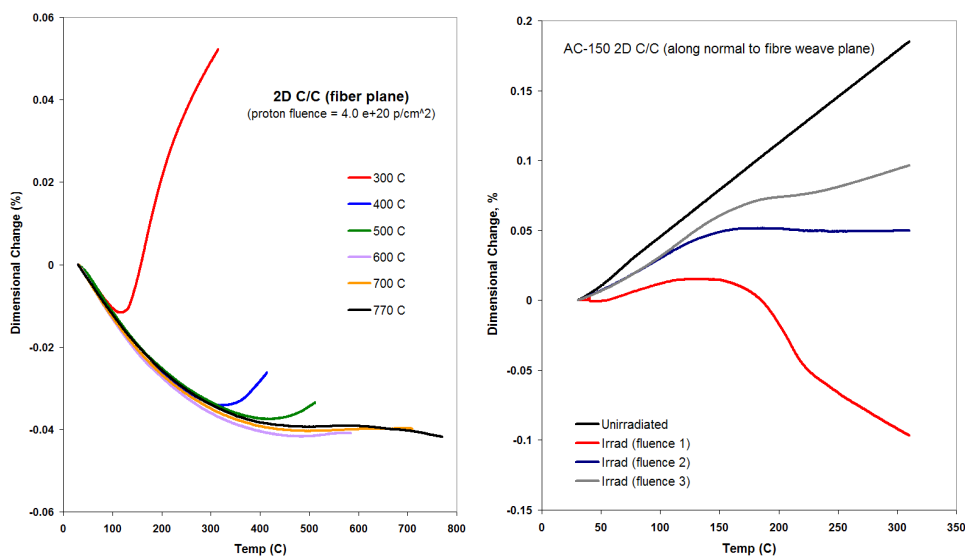
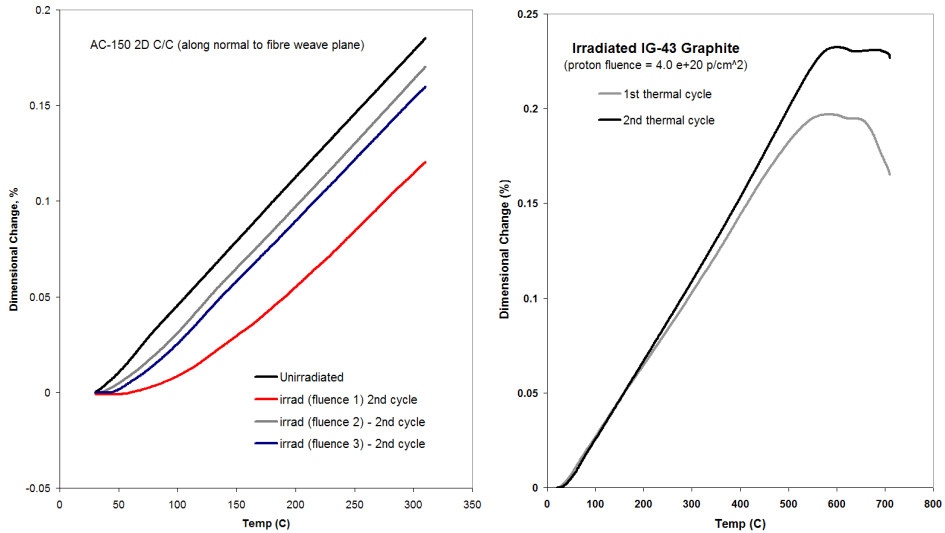


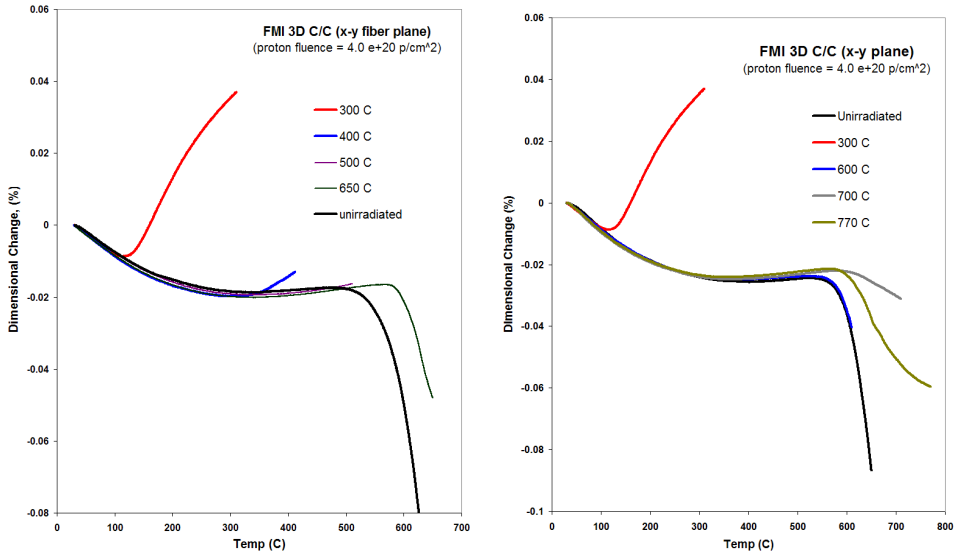
Fig. 9. Dimensional change in 2D C/C composite following proton irradiation and removal of fibre shrinkage (left) with thermal annealing in the fibre direction and growth (right) induced in lattice along the normal to fibre direction as a function of fluence (1 = $6.0 \cdot 10^{20}$ p/cm²; 2 = $3.0 \cdot 10^{20}$ p/cm²; 3 = $1.0 \cdot 10^{20}$ p/cm²)

1



2
3
4
5
6

Fig. 10. Restoration of growth along the normal direction of irradiated 2D C/C fibres through thermal cycling and as a function of proton fluence (left) and of irradiated IG-43 graphite irradiated with fluence $4.0 \cdot 10^{20} \text{ p/cm}^2$



7
8
9

Fig. 11. Dimensional change and thermal annealing of 3D C/C composite structures following proton irradiation with fluence $4.0 \cdot 10^{20} \text{ p/cm}^2$

10 The dimensional changes of irradiated 3D C/C composite are shown in Figure 11. For the 3D
11 architecture the material exhibits a negative CTE in all directions. As seen in Figure 11 for the

1 un-irradiated samples, there is accelerated shrinkage $>600^{\circ}\text{C}$ attributed to the influence of the
2 matrix within the fibre structure. Reversal from shrinkage to growth at these temperatures was
3 observed in previous studies (Burchell, 1994). Measurements of thermal conductivity of the
4 irradiated 3D C/C and IG-43 graphite samples following proton irradiation revealed that
5 thermal conductivity reduced by a factor of three (3) for the 3D C/C for 0.25 dpa fluence and
6 by a factor of six (6) for IG-43 and similar fluence. To address the significantly higher
7 irradiation damage from energetic protons a new irradiation experiment has been initiated
8 where the carbon composite will be exposed to a neutron flux at the BNL BLIP facility which
9 results from the spallation of protons with upstream isotope targets. The goal is to compare the
10 damage at similar fluences of energetic protons and energetic neutrons.

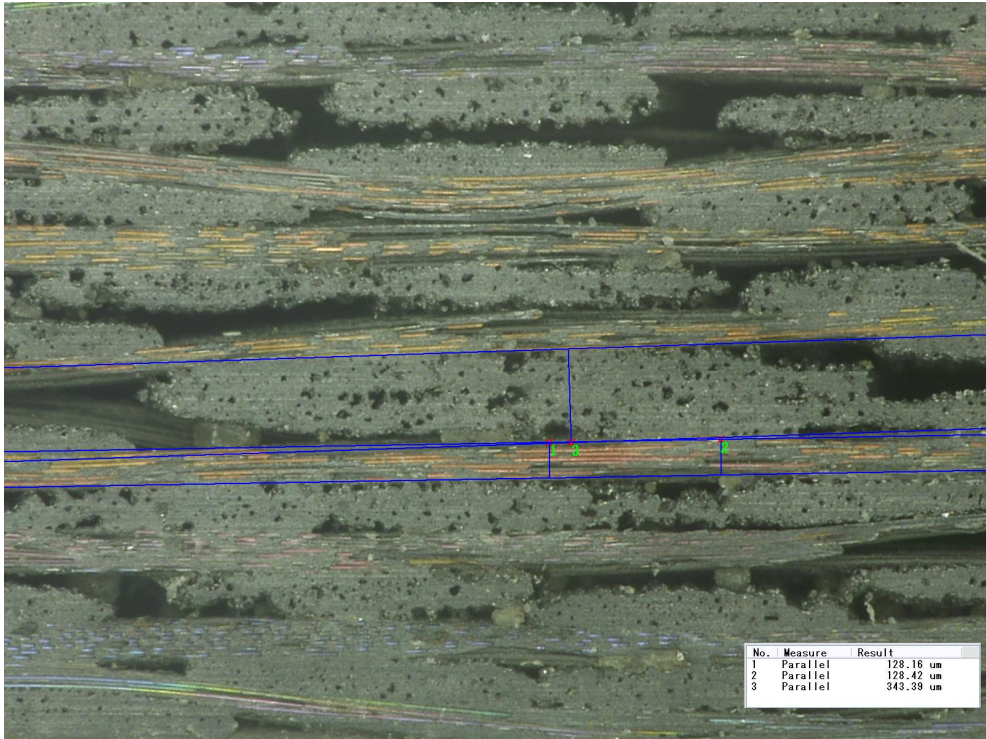
11 **2.2 SiC_f/SiC**

12 Silicon carbide fibre reinforced composites (SiC_f/SiC), along with the C/C composites,
13 considered as prime candidates for the first wall and blanket structural material in fusion
14 reactors. Due to their low activation and irradiation stability these composites have a clear
15 advantage over the C/C composites especially when the neutron doses are expected to be
16 high as it is the case of fusion reactors where tens of dpa over the lifetime will be
17 accumulated. Its inherent stability stems from the isotropic dimensional change of the
18 cubic SiC crystal (Bonal et al. 2009) which tends to saturate at modest irradiation levels. It
19 also exhibits good fracture resistance and excellent mechanical properties at high
20 temperatures. While the carbon composite technology and manufacturing is more mature
21 than that of the SiC composites, which currently have limited structural applicability
22 outside nuclear reactors. Significant progress has been made in recent years to both
23 eliminate issues of early grades of the composite associated with poor irradiation
24 performance (Snead et al., 1992) and reduce cost through adoption of novel fabrication
25 techniques (Katoh et al., 2010) such as the nano-infiltrated transient-eutectic (NITE) process
26 (Bonal et al., 2009). For nuclear grade SiC_f/SiC composites the costly chemical vapour
27 infiltration technique (CVI) is used.

28 To assess the neutron irradiation damage of SiC_f/SiC composites grades produced by a
29 variety of approaches a number of irradiation experiments have been launched using the
30 HFIR and JTMR reactors (Katoh et al., 2010). Irradiation of the various grades at HFIR to
31 levels up to 10 dpa and at elevated temperatures of 800°C has also been conducted. The key
32 objective is to assess the strength and stability of the improved composites and the thermal
33 conductivity degradation. In contrast to the early SiC_f/SiC grades which suffered significant
34 irradiation damage from de-bonding of fibre matrix interface driven by fibre densification
35 the new grades show minimal degradation of strength and stability of mechanical
36 properties up to 10 dpa (Katoh et al., 2007). Thermal conductivity, however, remains an
37 issue for low irradiation temperatures.

38 An experimental study on the effects of high temperatures and proton or fast neutron
39 irradiation has been initiated at Brookhaven National Laboratory. The goal is to subject
40 SiC_f/SiC composite to similar irradiation fields that the carbon composites have been
41 exposed to and make comparison in the irradiation-induced damage. As discussed in the
42 previous section, significant damage was observed in C/C composites at levels far below
43 the observed limits in neutron irradiation environments. Shown in Figure 12 is an optical
44 image of SiC_f/SiC composite section showing the fibre bundle thickness ($\sim 128\mu\text{m}$) and the
45 SiC matrix thickness ($\sim 343\mu\text{m}$). Also shown in Figure 12 is the distribution of voids within

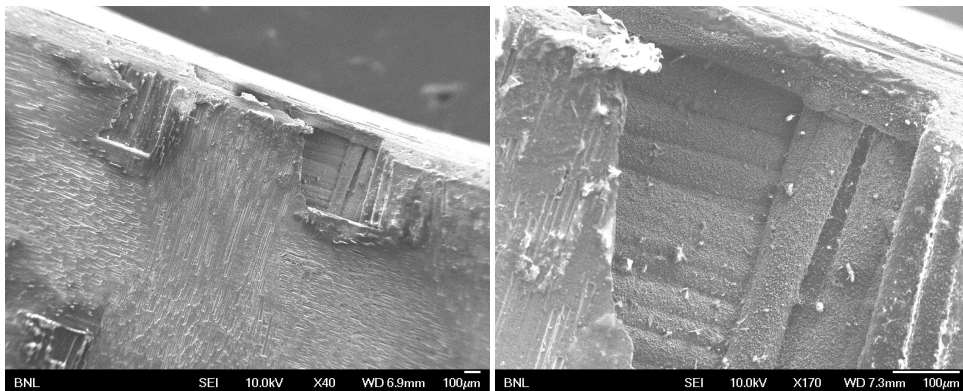
1 the architecture. Figures 13 and 14 are SEM images of the fibre/matrix interfaces and of the
 2 individual fibres.
 3



4
 5 Fig. 12. Optical microscope image of a SiC_f/SiC structure showing the arrangement of the
 6 weaved fibre bundles and the matrix

7 To assess the effect of high temperature on the SiC_f/SiC in terms of dimensional changes,
 8 structure and density composite samples were brought to 1000°C in atmosphere and the
 9 changes were made with precise instruments at the BNL isotope facility. Dimensional
 10 changes were more pronounced along the fibres (shrinkage of $\sim 1\%$) while in the direction
 11 normal to the fibres they were of the order of 0.09% . Density reduction of $\sim 0.8\%$ was also
 12 observed ($\rho_{\text{rt}} = 2.4324 \text{ g/cc}$) following the annealing of the sample for one hr at 1000°C .
 13 Shown if Figure 17 is dimensional changes obtained for temperatures up to 610°C and are
 14 compared with those of 3D C/C. As seen in Figure 17 during the first thermal cycle there is
 15 an adjustment in the both structures except more pronounced in SiC_f/SiC which expands
 16 with increasing temperature in contrast to C/C which shrinks for the selected temperature
 17 range. Based on the stabilized thermal expansion, the thermal expansion coefficient (CTE) in
 18 the range of $200\text{-}600^\circ\text{C}$ was estimated as $3.7 \cdot 10^{-6}/\text{K}$. Experimental results (Zhang, 2006)
 19 on carbon fibre reinforced SiC (via CVI method) up to 1400°C showed values similar average
 20 values in the $200\text{-}600^\circ\text{C}$ but with dramatic fluctuations above 800°C . Following the planned
 21 proton irradiation of the SiC_f/SiC and the fast neutron irradiation using the spallation
 22 process at the isotope production facility at BNL the effects on the physio-mechanical
 23 properties will be studied and compared with the C/C composites.

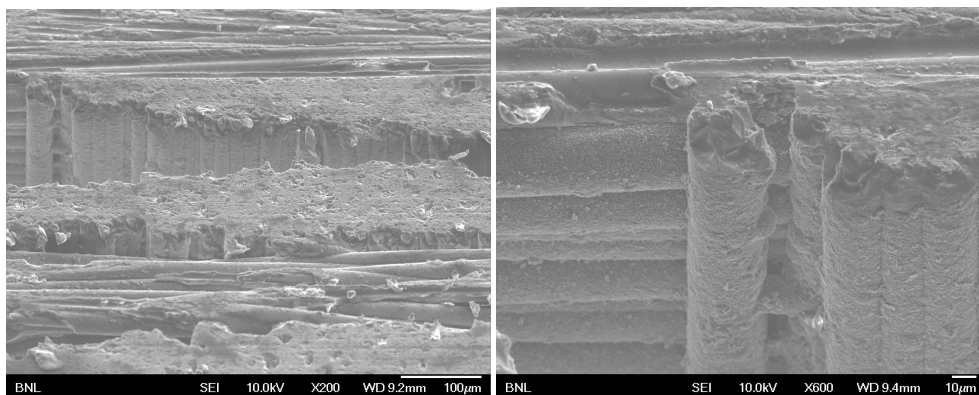
1



2

3 Fig. 13. SEM photograph of a SiC_f/SiC cut section (left) and of fibre arrangement (right)

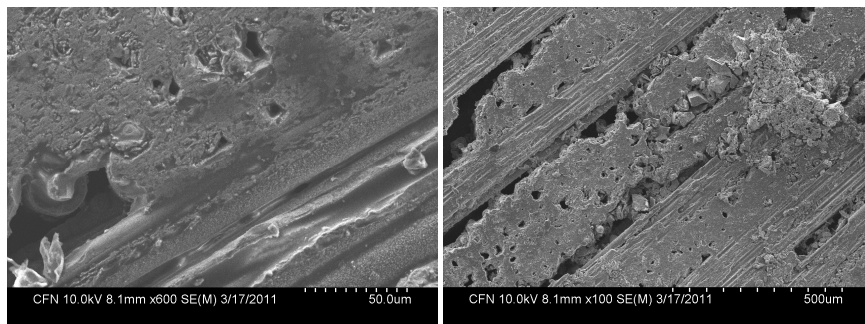
4



5

6 Fig. 14. SEM photograph of a fibre bundle (left) and fibre detail (right) of SiC_f/SiC

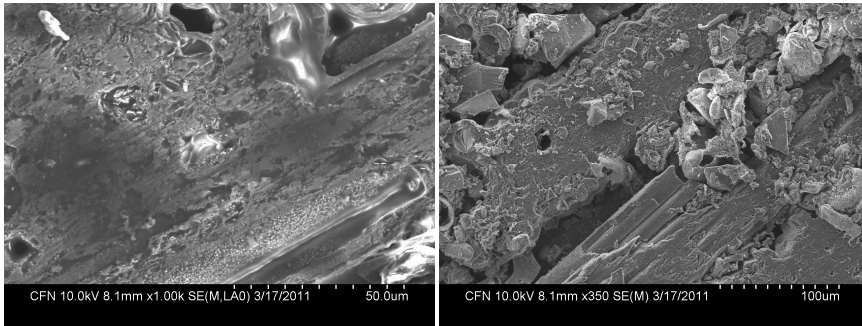
7



8

9 Fig. 15. SEM of a SiC_f/SiC section at room temperature (left) and following annealing at
10 1000°C for one hour (right)

1



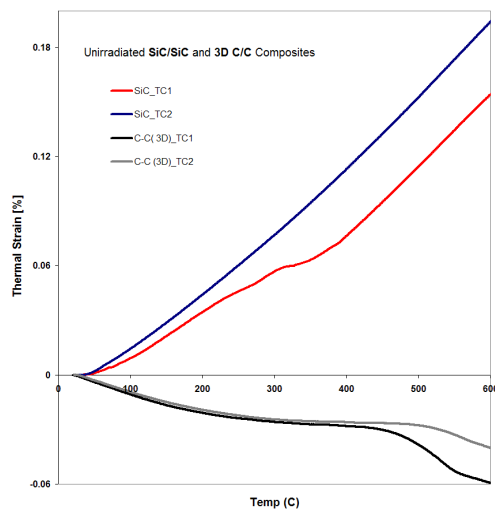
2

3

4

5

Fig. 16. Close SEM view of a SiC/SiC section at room temperature (left) and following annealing at 1000°C for one hour (right)



6

7

8

Fig. 17. Dimensional change of un-irradiated SiC/SiC composite over two thermal cycles (noted as TC1 and TC2) and comparison with 3D C/C

9

2.3 Composite-like structures

10

11

12

13

14

15

16

17

18

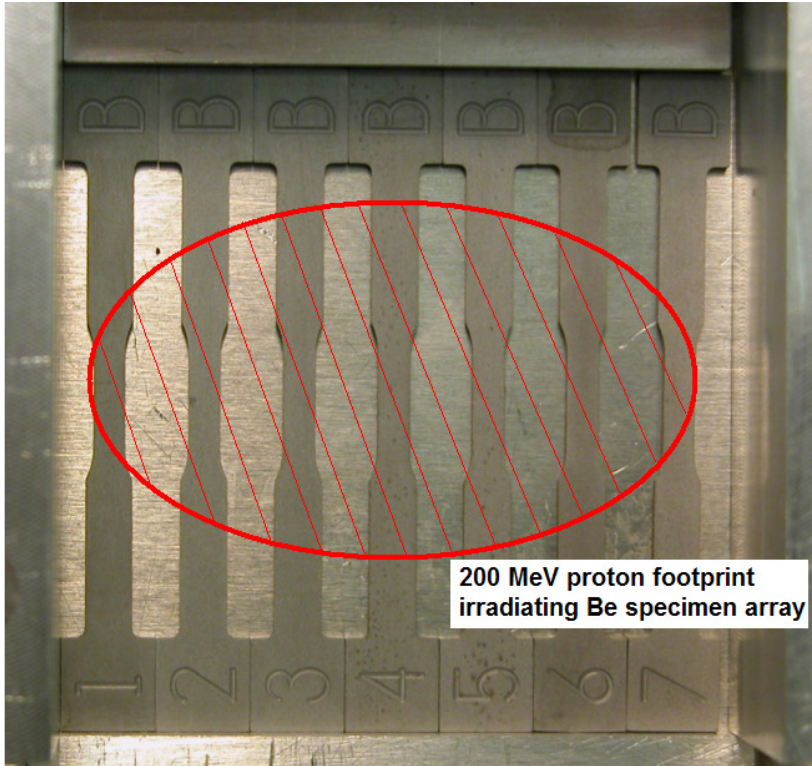
A number of material structures not adhering to the classical definition of composites involving a matrix with fibre-reinforcement, i.e. C/C, C/SiC, SiC_i/SiC, etc., can still be considered composites, or more appropriately composite-like with potential applications in the next generation fusion and fission nuclear reactors. These can be based on (a) the embedment of particles of one material into the lattice of another thus maintaining the individual characteristics, (b) the bonding of dissimilar materials using solid state reaction of chemical vapour deposition with the help of an interface layer, and (c) on deposition of nano-structured coatings on substrates to either enhance the properties of the combined structure or protect the substrate. Because of their potential for use in nuclear reactors, some

1 of these composite-like structures have been studied for radiation damage and extreme
2 temperatures.

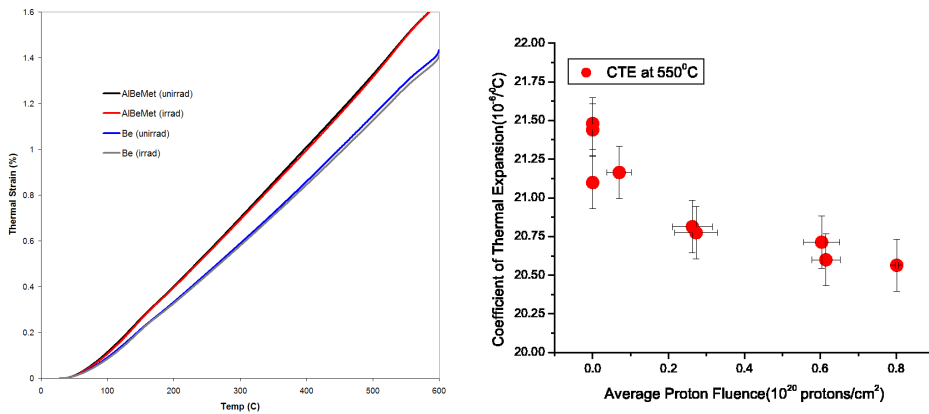
3 **2.3.1 AlBeMet**

4 AlBeMet, while by metallurgical definition may be considered an alloy, is in fact a
5 composite of aluminium and beryllium consisting typically of ~62% commercially pure
6 beryllium and 38% of commercially pure aluminium by weight. The two metals involved in
7 forming AlBeMet do not fully mix but instead the beryllium particles are embedded in a
8 pure aluminium lattice. The powder is produced by a gas atomization process yielding a
9 fine beryllium structure. The two granular forms are mixed at temperatures just below the
10 melting points of the two metals and a pressure that prompt the particles to form a stable
11 bond. The result is a non-typical composite with some very appealing thermo-physical
12 properties since it combines the workability of aluminium and, for the most part, the
13 hardness of beryllium. Interest in this special composite has been increased in recent years
14 primarily for use in special components of particle accelerator systems and in particular in
15 the accelerator target envelope characterized by high-radiation, high temperature and
16 thermal shock conditions. The combination of low-Z, good thermal conductivity (210 W/m-
17 K) and low electrical resistivity (3.5e-6 Ohm-cm), combined with its workability and
18 hardness, make it very attractive for special components such as magnetic horns and targets.
19 Unknown was its radiation resistance and dimensional stability which are key parameters
20 for potential applications in nuclear reactor systems. The effects of radiation on the physical
21 and mechanical properties of this unique composite have been studied using direct
22 energetic protons and secondary fast neutrons of the BNL accelerator complex through a
23 series of irradiation experiments. Peak proton fluences of $3.0 \cdot 10^{20}$ p/cm² at 140 MeV using
24 the 200 MeV proton beam at BNL BLIP and, through a different study, fast neutron fluences
25 of $\sim 10^{19}$ n/cm² were achieved in these accelerator-based irradiation experiments. The
26 arrangement of specially designed test samples of beryllium (similar to AlBeMet samples) in
27 the irradiation space intercepting the proton beam is shown in Figure 18. The numbered
28 tensile specimens (dog-bone) are 42mm long and 1.5mm thick and have a strain gauge
29 length of 6mm. The matching specimens are used for post-irradiation analysis of thermal
30 expansion, electrical and thermal conductivity.

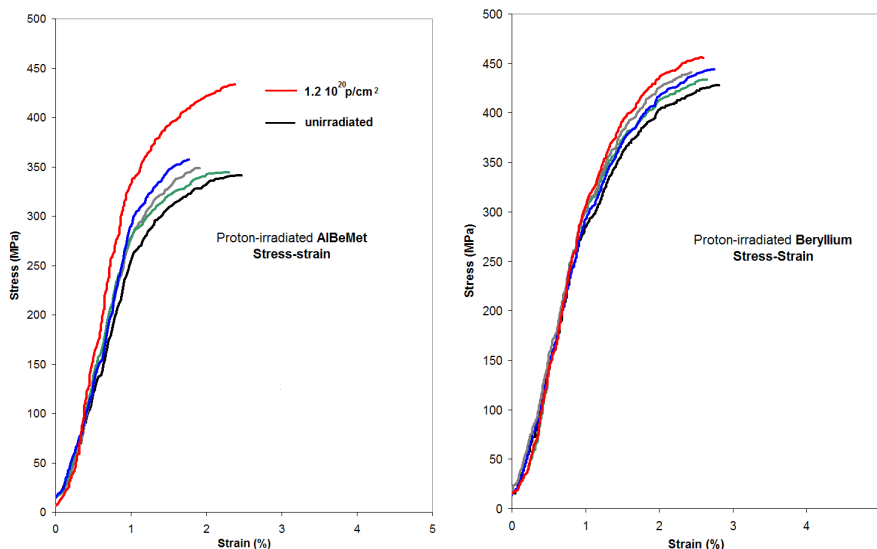
31 Post-irradiation studies revealed that AlBeMet is dimensionally stable following irradiation
32 and that it resists embrittlement and degradation even at high proton fluences where
33 materials such as graphite and carbon composites have shown to undergo serious
34 degradation. As indicated above, the proton fluences received may be representative of a
35 much more severe irradiation condition when correlated to either thermal or fast neutrons.
36 Depicted in Figure 19 is the thermal expansion of both AlBeMet and beryllium for peak
37 fluence of $1.2 \cdot 10^{20}$ p/cm² and the measured CTE of AlBeMet as a function of average proton
38 fluence. The effects of proton irradiation on the stress-strain relation of AlBeMet and its
39 comparison with beryllium are shown in Figure 20. While it is confirmed that the ultimate
40 tensile strength of beryllium is higher than that of AlBeMet, the AlBeMet appears to increase
41 its strength following irradiation (as expected in all metals due to the pinning of
42 dislocations) but without loss of the ductility anticipated to accompany the induced
43 hardening. Further tests are planned where AlBeMet will be exposed to higher proton and
44 accelerator-produced fast neutron fluences to explore its mechanical behaviour.



1
2 Fig. 18. Arrangement of irradiated test samples of beryllium intercepting the 200 MeV
3 proton beam at BNL isotope production facility.
4



5
6 Fig. 19. Thermal expansion (left) comparison of AlBeMet and beryllium irradiated by 200
7 MeV protons and peak fluence of $1.2 \cdot 10^{20}$ p/cm², and coefficient of thermal expansion of
8 AlBeMet (right) at 550°C as a function of proton fluence



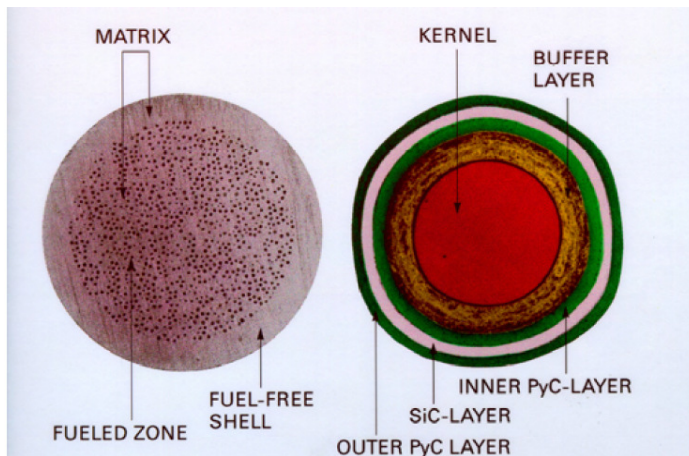
1
2 Fig. 20. Effects of 140 MeV proton irradiation on AlBeMet (left) and beryllium (right) on the
3 stress-strain relations (range of fluence of irradiated samples $0.4 - 1.2 \cdot 10^{20} \text{ p/cm}^2$)

4 2.3.2 Bonded dissimilar materials

5 Bonding of dissimilar materials to create a “composite-like” structure and ensuring its
6 ability to maintain the integrity of the interfaces under extreme temperature conditions and
7 high radiation fluences is an important challenge. Applications of such composites can be
8 seen in nuclear fuel elements, fusion reactor plasma facing components where high-Z
9 materials such as tungsten with higher erosion resistance will protect low Z materials like
10 carbon or beryllium and particle accelerator targets where the variation of the material
11 atomic number Z from the centre of the intercepted beam is important for both particle-mass
12 interaction and heat removal from the hot central part (Simos et al., 2006b). In all
13 applications and due to the dissimilarity of the thermal expansion in the bonded material
14 structure, high stresses can develop at the interfaces leading to micro-cracking or even
15 separation. Such condition can dramatically reduce a key property of the composite layer
16 that controls the primary function such as heat transfer across the interfaces through
17 thermal conduction. Shown in Figure 21 is a schematic of a TRISO-coated particle and
18 pebble bed fuel sphere for Generation-IV Very High Temperature Reactor (VHTR).
19 Maintaining the integrity of the interfaces between the various layers around the fuel kernel
20 under high temperatures and extreme radiation fluxes is crucial. The dimensional changes
21 occurring as a result of the two simultaneous effects do not necessarily coincide in terms of
22 direction (growth or shrinkage) and thus a better understanding of the interface mechanics
23 under such conditions is required.

24 There is a significant need in the nuclear industry and in particular in the first wall of fusion
25 reactors, of graphite/metals bonding to form a coating or cladding on the low Z materials
26 (i.e. graphite) and reduce the erosion rate. Direct graphite-metal junctions (Brossa et al.,
27 1992) for use in the first wall of fusion reactors are extremely sensitive to thermal cycling

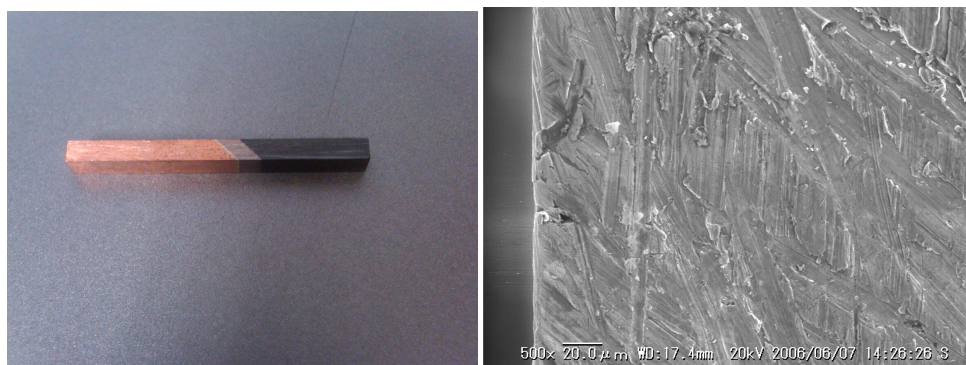
1 due to differences in thermal expansion so techniques have been developed and applied
 2 with the introduction of interface agents (such as silver) that will prevent the formation of
 3 fragile components and metal dissolution. Thus brazing between stainless steel and
 4 graphite, Mo and graphite as well as W and graphite has been produced using vacuum
 5 plasma spray (VPS) and chemical vapour deposition (CVD) techniques. To study the
 6 resilience to thermal shock, graphite/Mo or graphite/W bonding was achieved by using an
 7 intermediate layer of Mo, V, or Mo-Ti and applying a solid state reaction bonding technique
 8 (Fukatomi et al., 1985).
 9



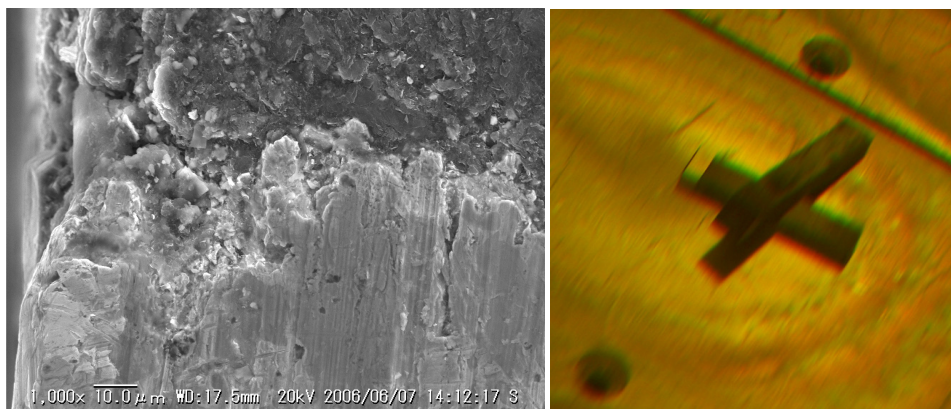
10
 11 Fig. 21. TRISO-coated particle and fuel element for a pebble bed reactor (US DOE, 2006)

12 To assess the effect of proton irradiation bombarding the muon target at J-PARC facility
 13 where a 3 GeV, 333 μA proton beam is intercepted by a graphite target at a rate of 25 Hz an
 14 experimental study was initiated at Brookhaven National Laboratory. The study consisted
 15 of an irradiation phase using the 200 MeV proton beam of the BNL Linac and of a post-
 16 irradiation analysis to observe the degradation of the target-like composite structure that
 17 was made for the study. Shown in Figure 22 is a test specimen consisting of three materials
 18 (copper and titanium alloy Ti-6Al-4V) and graphite (IG-43) and two interfaces (graphite to
 19 titanium and copper to titanium alloy). To form the two interfaces the silver brazing
 20 technique in vacuum was applied. Two types of geometry in the 42mm long (4mm x 4mm
 21 cross sectional area) specimens was used, one at 45° (as shown) and one with normal or 90°
 22 interfaces. Shown in the SEM image of Figure 22 and prior to irradiation is the achieved
 23 bonding/interface (extremely faint) between copper and titanium alloy for the 90° interface.
 24 The composite specimens were placed in the proton beam and received peak fluence over
 25 the two interfaces of $\sim 8.0 \cdot 10^{20}$ p/cm². Post-irradiation examination revealed the loss of
 26 integrity of the graphite/copper interface and the complete separation. Shown in Figure 23
 27 is the graphite-to-titanium interface zone prior to irradiation and the condition of the
 28 composite structure after irradiation. As it has been assessed by focussing on the graphite
 29 susceptibility to high energy proton irradiation (elevated irradiation damage due to the
 30 nuclear interactions and the accelerated formation of He bubbles trapped in the lattice) as
 31 part of the same irradiation study, the degradation of the interface is attributed to graphite
 32 radiation damage. The composite dimensional changes, which will inevitably result in

1 interface stresses due to thermal expansion coefficient differences, were studied by
 2 analyzing the thermal strain as a function of temperature using the high-sensitivity
 3 dilatometer in the hot cell. Shown in Figure 24 are the thermal expansion of the composite
 4 structure (graphite/copper/titanium) for both 45 and 90-degree interface orientations and
 5 the three components of the composite when all have received the same proton fluence. The
 6 dissimilar rates of expansion between the three constituents and the dimensional change
 7 reversal of graphite above 600°C (discussed previously) introduce a non-linear thermal
 8 expansion trace. Important to note is that subsequent thermal cycles above the 600°C
 9 threshold, resulted in a complete failure and fracturing of the irradiated graphite in the
 10 composite. This was observed for both interface orientations and attributed to the growth
 11 reversal in the graphite leading to fracture of an already compromised graphite strength
 12 resulting from radiation damage.
 13



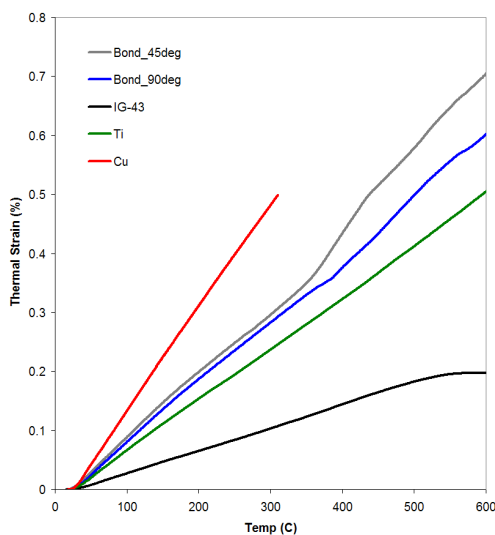
14
 15 Fig. 22. Graphite-titanium-copper composite sample (left) used for the BNL irradiation
 16 studies and SEM image of the copper-titanium interface prior to irradiation



17
 18 Fig. 23. SEM image (left) of the graphite (top) and titanium interface prior to the 200 MeV
 19 proton irradiation and image of the degraded interface following irradiation (right)

20 The study demonstrated the serious effects that energetic protons at fluences above $\sim 5.0 \cdot 10^{20}$
 21 protons/cm² have on graphite and thus its interface or bonding with metals. In the fusion

1 reactor, however, composite structures that involve graphite with metal cladding or coating
2 will be exposed to higher fluences of 14 MeV fast neutrons. While for such neutron energies
3 it is anticipated that the cross section of nuclear interaction is similar to that of the 200 MeV
4 protons, confirmatory investigations are necessary. It should be emphasized that nuclear
5 graphite exposed to higher fluences of thermal neutrons (< 1 MeV) than the ones achieved
6 with the 200 MeV protons has shown much greater resilience to irradiation damage.
7 Therefore, to address the potentially different response of such graphite to metal bonding
8 experiment using the spallation-produced fast neutrons at the BNL isotope facility has been
9 launched. During this irradiation phase fast neutron fluences of $\sim 2.0 \times 10^{19}$ n/cm² and
10 dominated by energies between 1 MeV and 30 MeV will be achieved. While these levels are
11 far below the fusion reactor fluences anticipated for the graphite/metal composite
12 structures, a comparison between proton and neutron irradiation at similar exposure levels
13 can be made.
14
15



16
17 Fig. 24. Thermal strain of the composite structures and of the three constituents all exposed
18 to the same level of proton fluence ($\sim 2.0 \times 10^{20}$ protons/cm²).

19 2.3.3 Nanostructured coatings

20 While nano-structured coatings on metal substrates form a unique class of materials with a
21 wide range of applications, the combined coating/substrate structure can be also
22 characterized as a composite. These structures exhibit similar behaviour at the interface
23 between the substrate and the coating as fibre-reinforced matrices stemming from the
24 mismatch of thermal expansion coefficient which leads to elevated interface stress fields at
25 high temperatures. With recent advances in the techniques and application of nanocoatings
26 on base materials such as thermal spray deposition (Tsakalakos, 2009), interest has increased
27 for their potential use in nuclear reactor systems and in particular in plasma-facing
28 components of fusion reactors.

1 In fusion reactor environments where the low Z materials of the plasma-facing wall (carbon
2 or beryllium) require protection from erosion, coatings based on tungsten and its alloys
3 have been explored (Koch, 2007). In such setting, however, extreme radiation damage
4 presents an additional challenge for these relatively untested structures which alters the
5 physio-mechanics of the interaction between the substrate and the coating due to the fact
6 that the rate of change of the thermal expansion (CTE) as a function of the radiation fluence
7 may differ significantly between the distinct materials. Therefore, the potential for micro-
8 cracking and even separation between the substrate and the coating under a combination of
9 extreme temperatures and radiation fluxes requires experimental investigation.

10 Experimental studies focussing on the radiation and extreme temperature effects on alumina
11 (Al_2O_3) and titania (TiO_2) nano-structured coatings applied on Ti-6Al-4V and 4130 steel alloy
12 substrates were launched to assess their susceptibility. Specifically, 200 μm -thick coatings
13 consisting of 87% Al_2O_3 and 13% TiO_2 (grid-blasted) and 600 μm -thick Al_2O_3 (thermally
14 sprayed) on Ti-6Al-4V substrates were used along with 600 μm -thick Al_2O_3 and 600 μm -thick
15 amorphous Fe coating on alloy steel 4130 substrates. The behaviour of the interface of the
16 between the substrate and the coating was evaluated for temperatures reaching 1200°C. In
17 addition, the radiation damage from the spallation-based radiation field at BNL BLIP using
18 116 MeV protons. During irradiation, nano-coated samples received a neutron fluence of
19 $\sim 2.0 \times 10^{19}$ n/cm² with mean energy of 9 MeV. Combined with the neutron fluence, the
20 coatings received a secondary proton fluence of $\sim 3.2 \times 10^{15}$ p/cm² of 23 MeV mean energy, a
21 photon fluence of $\sim 3.0 \times 10^{19}$ γ /cm² of 1 MeV mean energy and $\sim 2.4 \times 10^{16}$ e/cm² of 1 MeV
22 mean energy. Of primary interest was the effect of irradiation on the thermo-mechanical
23 behaviour of the structures. Shown in Figure 25 are changes that occur at the interface of
24 600 μm -thick Al_2O_3 on Ti-6Al-4V substrate from room temperature, to 900°C and 1200°C.
25 Demonstrated is the resilience of the composite structure despite the high interface stresses
26 which result in shear failure planes in the substrate (middle image). At higher temperatures
27 (1200°C) the substrate material begins to re-arrange across the shear failure plane. The effect
28 of extreme temperatures on the 600 μm -thick Al_2O_3 layer deposited on alloy steel 4130
29 substrate is quite different as shown in Figure 26. At elevated temperatures (>600°C) an
30 inter-metallic layer begins to form at the interface eventually leading to complete separation
31 of the nano-structured alumina layer at 1200°C.



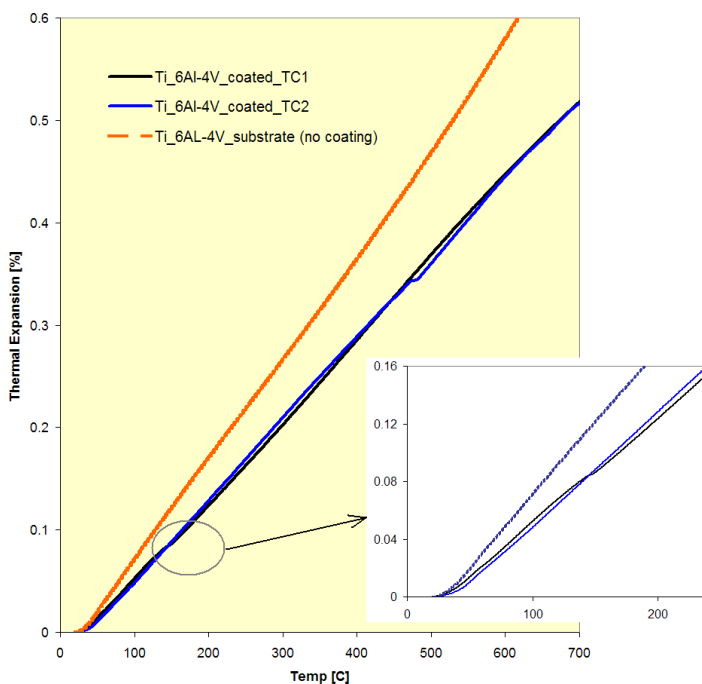
33
34 Fig. 25. Effect of temperature on the interface of nano-structured alumina coating on Ti-6Al-
35 4V substrate from room temperature (left), to 900°C (middle) and 1200°C (right)

36 The effects of irradiation on the thermal expansion of the coated samples were studied and
37 are depicted in Figures 27 and 28 where they are compared with their un-irradiated
38 counterparts. Observed in the un-irradiated case is that the coating and substrate adjust at
39 certain temperatures to accommodate for the dissimilarities in thermal expansion

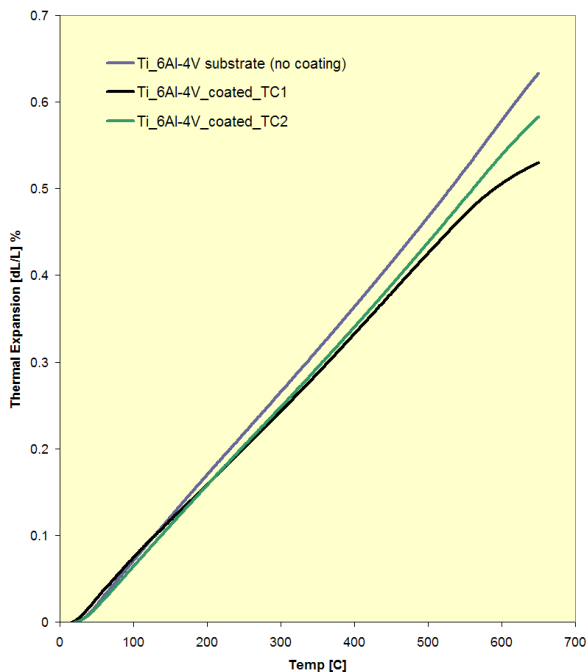
1 coefficient. The adjustment which first occurs at a low temperature ($\sim 150^\circ\text{C}$) re-occurs at a
 2 higher temperature in a subsequent thermal cycle. This behaviour in which the two
 3 dissimilar materials adjust at a particular temperature is very similar to what has been
 4 observed near phase transitions in bcc metals such as tungsten. The radiation effects on the
 5 stress-strain behaviour based on specially-designed and irradiated specimens with the
 6 fluences mentioned above are currently being evaluated.
 7



8
 9 Fig. 26. Effect of temperature on the interface of nano-structured alumina coating on 4130
 10 steel alloy substrate from room temperature (left), to 900°C (middle) and 1200°C (right)
 11



12
 13 Fig. 27. Thermal expansion of Ti-6Al-4V substrate coated with $200\mu\text{m}$ -thick Al_2O_3 - TiO_2
 14 layer compared with the thermal expansion of the substrate alone for the same temperature
 15 range. Shown is the re-adjustment that takes place in the coated sample at different
 16 temperatures in the thermal cycles (TC1=1st thermal cycle, TC2=2nd thermal cycle).



1
2 Fig. 28. Thermal expansion of Ti-6Al-4V substrate coated with 200 μm -thick Al_2O_3 - TiO_2
3 layer compared with the thermal expansion of the substrate alone for the same temperature
4 range following irradiation with neutrons of fluence $2.0 \text{ e}+19 \text{ n/cm}^2$.

5 3. Conclusion

6 With the development of the new generation composites such as C/C, and SiC/SiC as well
7 as special bonds and coatings rapidly advancing and, in the process, performance in
8 extreme environments is better understood and quantified, there is high degree of
9 confidence that these material structures will be able to support the needs of the next
10 generation reactors. A multitude of efforts world-wide have been aiding in closing the
11 knowledge gap on these very promising materials during the last three decades while, with
12 the adoption of novel processing techniques, have made their fabrication at a large-scale
13 feasible. However, due to the harshness of the nuclear environment of the future reactors,
14 consisting of a combination of extremes in temperature and radiation flux, further work is
15 necessary to qualify these composites since the available data are the results of small-scale
16 experimental efforts. The extensive experience on the constituents of these composites from
17 fission reactors may not necessarily provide a good basis to assess the performance of the
18 integrated composite in the elevated nuclear environments. As some of the irradiation
19 experiments using more energetic particles than the thermal neutrons from fission reactors
20 on materials with well understood behaviour (i.e. graphite) showed is that irradiation-
21 induced damage may occur at a faster rate at much lower thresholds. This emphasizes the
22 need to understand and quantify the performance of both the constituents and the final
23 composite structure under prolonged exposure to higher energy neutrons that make up the
24 flux in the next generation fusion and fission reactors.

1 Irradiation damage studies to-date focussing on the next generation composites and using
2 the available facilities have shown that it is feasible with these new material forms to
3 achieve the performance required through extrapolation. However, the actual conditions in
4 the fusion and next generation fission reactors are expected to be more severe in terms of
5 flux, fluence and temperature. These may result in a much greater spectrum of changes in
6 the physio-mechanical properties of these materials especially in hydrogen and helium
7 formation. The knowledge of the behaviour of these promising composite materials at these
8 levels, either extrapolated or acquired through tests simulating the anticipated conditions,
9 will still be at a small scale. For application in the large-scale of the fusion or fission reactor
10 environment the small-scale must be extrapolated to the realistic size of the components.
11 Therefore a better handle of the scaling must be achieved with the development and
12 implementation of numerical codes. Because of the variability within their structure the
13 numerical models need to consider spatial variation of the properties. Code benchmarking
14 efforts focussed in the specifically on the prediction of the response of these composites will
15 be necessary. Important attributes that make these composites attractive, such as shock
16 resistance, need special attention and further experimental work due to the enormous
17 complexity of the problem associated with fibre-reinforced composites. The effect of
18 irradiation on the degradation of the physical and mechanical properties that control the
19 response to shock absorption, for example, down to the interface between the fibre and the
20 matrix need to be understood so the performance of the bulk composite can be assessed.

21 **4. Acknowledgment**

22 The author gratefully acknowledges the input of Dr. H. Ludewig for discussions on the
23 subject and for reviewing and commenting on the manuscript, Dr. L. Snead for providing
24 SiC/SiC samples for the study and Prof. T. Tsakalakos for providing the nanostructured
25 coating samples and for discussions on the subject. The help of A. Kandasamy, Dr. A. Stein
26 and Dr. J. Warren for facilitating the optical microscopy and SEM images is much
27 appreciated and acknowledged.

28 **5. References**

- 29 Barabash, V., Akiba M., Bonai J., Federici, G., Matera, R., Nakamura, K., Pacher, D., Rodig,
30 M., Vieder, G., & Wu, H. (1998). Carbon fibre composites application in ITER
31 plasma facing components. *Journal of Nuclear Materials*, Vol. 258-263, P, pp. 149-
32 159
- 33 Bonal, J-P., Kohyama K., van der Laan J & Snead L. (2009). Graphite, Ceramics and Ceramic
34 Composites for High-Temperature Nuclear Power Systems. *MRS Bulletin*, Vol. 34,
35 pp. 28-34
- 36 Brossa, F., Franconi E. & Schiller P. (1992). Development of graphite/metals bondings for
37 fusion reactors applications. *Journal of Nuclear Materials*, Vol. 191-194, pp. 469-472
- 38 Burchell, T. (1994). Irradiation-induced structure and property changes in tokamak plasma-
39 facing, carbon-carbon composites. *Proceedings of the 39th International
40 Symposium of the Society for the Advancement of Material and Process
41 Engineering and Exhibition, Anaheim, CA, April 1994*
- 42 Burchell, T. (1996). Radiation Damage in Carbon-Carbon Composites: Structure and
43 Property Effects. *Physica Scripta*, Vol. T64, pp. 17-25

- 1 Burchell, T., Eatherly, P., Robbins, M. & Strizak P. (1992). The effect of neutron irradiation on
2 the structure and properties of carbon-carbon composite materials. *Journal of*
3 *Nuclear Materials*, Vol. 191-194 Part 1, pp. 295-299
- 4 Fukatomi, M., Fujitsuka, M. & Okada, M. (1985) The development of graphite/metal bonds
5 for fusion reactor applications, *Journal of Nuclear Materials*, Vol. 133-134, pp. 769-
6 772
- 7 Gittus, J.H., (1975). *Creep, Viscoelasticity and Creep Fracture in Solids*, Halsted Press, ISBN
8 0-470-30265-8, New York, USA
- 9 Goto, K. & Kagawa Y. (1996). Fracture behaviour and toughness of a plane-woven SiC fibre-
10 reinforced SiC matrix composite. *Materials Science and Engineering A211*, pp. 72-
11 81
- 12 Hereil, P.-L., Allix, O. & Gratton, M. (1997). Shock Behaviour of 3D Carbon-Carbon
13 Composite. *Journal Phys IV France*, Vol. 7, pp. 529-534
- 14 Jones, H., Steiner D., Heinisch H.L., Newsome A. & Kerch M. (1997). Radiation resistant
15 ceramic matrix composites. *Journal of Nuclear Materials*, Vol. 245, pp. 87-107
- 16 Katoh, Y., Snead, L., Nozawa, T., Kondo, S. & Busby, T. (2010a). Thermophysical and
17 mechanical of near-stoichiometric fiber CVI SiC/SiC composites after neutron
18 irradiation at elevated temperatures. *Journal of Nuclear Materials*, Vol. 403, Issues
19 1-3, pp. 48-61
- 20 Katoh, Y. Nozawa, T., Snead, L. & Hinoki T. (2010b). Effect of neutron irradiation on tensile
21 properties of unidirectional silicon carbide composites. *Journal of Nuclear*
22 *Materials*, Vol. 367-370, pp. 774-779
- 23 Koch, F. & Bolt, H. (2007). Self passivating W-based alloys as plasma facing materials for
24 nuclear fusion. *Physica Scripta*, Vol. T128, pp. 100-105
- 25 Kohyama, A., Hasegawa, A., Noda, T. & Katoh, Y. (n.d.). Present status of SiCf/SiC
26 composites as low-activation structural materials of fusion reactors in Japan. IAEA-
27 F1_CN-69/FTP/37, pp. 2-5
- 28 Nikolaenko, A., Karpukhin, I., Kuznetsov, N., Platonov A., Alekseev, M., Chugunov, K.,
29 Stronmbakh, I., Baldin, D., Rodchenkov, S., Smirnov, I, Subbotin, V., Khadomirov,
30 E. & Lebedev, G. (1999). Effect of the composition of radiation on the radiation
31 damage to graphite. *Atomic Energy*, Vol. 87, No. 1, pp. 480-484
- 32 Maruyama, N. & Harayama M. (1992). Neutron irradiation effect of thermal conductivity
33 and dimensional change of graphite materials. *Journal of Nuclear Materials*, Vol.
34 195, pp. 44-50
- 35 Simos, N., Kirk, H., Thieberger, P., Ludewig, H., Weng, W.-T., Trung P.-T., McDonald, K.,
36 Sheppard, J., Yoshimura, K. & Hayato, Y. (2006a). Solid Target Studies for Muon
37 Colliders and Neutrino Beams. *Nuclear Physics B – Proceedings Supplements*, Vol.
38 155, Issue 1, pp. 288-290
- 39 Simos, N., Kirk, H., Thieberger, P., Ludewig, H., Weng, W.-T., Trung P.-T., McDonald, K.,
40 Sheppard, J., Evangelakis, G., & Yoshimura, (2005). Target material irradiation
41 studies for high-intensity accelerator beams. *Nuclear Physics B – Proceedings*
42 *Supplements*, Vol. 149, pp. 259-261
- 43 Simos, N., Kirk, H., Thieberger, P., Ludewig, H., Weng, W.-T., Trung P.-T., McDonald, K.,
44 Sheppard, J., Yoshimura, K. & Hayato, Y. (2006a). Solid Target Studies for Muon
45 Colliders and Neutrino Beams. *Nuclear Physics B – Proceedings Supplements*, Vol.
46 155, Issue 1, pp. 288-290

- 1 Simos, N., Kirk, H., Ludewig, H., Mausner, L., O Connor J., Makimura, S. Yoshimura K., ,
2 McDonald, K., & Trung, P-T. (2006b). Material irradiation damage studies for high
3 power accelerators. Proceedings of EPAC'06, Edinburg, Scotland, June 2006, pp.
4 1816-1818
- 5 Simos, N., Kirk, H.G., Thieberger, P., Ludewig, H., O Connor, J., Mausner, L. Trung P-T.,
6 McDonald, K., Yoshimura, K. & Bennett, R. (2008). Irradiation damage studies of
7 high power accelerator materials. Journal of Nuclear Materials, Vol. 377, Part 1, pp.
8 41-51
- 9 Simos, N., Kirk, H., Ludewig, H., Mausner, L., O Connor J., Makimura, S. Yoshimura K., ,
10 McDonald, K., & Trung, P-T. (2006b). Material irradiation damage studies for high
11 power accelerators. Proceedings of EPAC'06, Edinburg, Scotland, June 2006, pp.
12 1816-1818
- 13 Snead, L., Steiner D. & Zinkle S. (1992). Radiation resistant ceramic matrix composites.
14 Journal of Nuclear Materials, Vol. 191-194, pp. 566-570
- 15 Snead, L. (2004). Ceramic structural composites. The most advanced structural material.
16 Presentation at the International School on Fusion Reactor Technology, Erice, Italy,
17 July 26 - August 1
- 18 Tsakalakos, T. (2009). Nanostructured Coatings & their Characterization under Nuclear
19 Energy System Extremes: Energy Dispersive X-ray Diffraction (EDXRD)
20 Synchrotron Probe. Presentation at Characterization of Advanced Materials under
21 Extreme Environment of the Next Generation Energy Systems Workshop,
22 Brookhaven National Laboratory, USA, September 25-26
- 23 Ullmaier, H. & Carsughi F. (1995). Radiation damage problems in high power spallation
24 sources. Nuclear Instruments and Methods in Physics Research B, Vol. 101, pp. 406-
25 421
- 26 US Department of Energy (2006), Basic Research Needs for Advanced Nuclear Energy
27 Systems, Available from: www.sc.doe.gov/bes/reports/files/ANES_rpt.pdf
- 28 Zhang, Q., Cheng L., Zhang L. & Xu Y (2006). Thermal expansion behaviour of carbon fibre
29 reinforced chemical-vapor-infiltrated silicon carbide composites from room
30 temperature to 1400oC. Materials Letters, Vol. 60, pp. 3245-3247
- 31 Zinkel, S. & Ghoniem N.M. (2000). Operating temperature windows for fusion reactor
32 structural materials. Fusion Engineering and Design, Vol. 51-52, pp. 55-71
- 33 Zinkle, J. (2004). Advanced Materials for Fusion Technology. Proceedings of the 23rd
34 Symposium on Fusion Technology, Venice, Italy, September 2004